

AI-Powered CNN Model for Automated Lung Cancer Diagnosis in Medical Imaging

Walid Ayadi¹, Yasser Farhat^{2,*}, Saeed Ali Althabahi¹, Nithiya Baskaran³, Showkat A. Dar⁴, R. Indhumathi⁵, Madhuri Prashant Pant⁶, Showkat A. Bhat⁷ and Aafaq A. Rather⁸

¹*Mechatronics and Intelligent Systems, Abu Dhabi Polytechnic, UAE*

²*Academic Support Department, Abu Dhabi Polytechnic, Abu Dhabi, UAE*

³*Department of Computer Science and Engineering, Chennai Institute of Technology, Tamil Nadu, India*

⁴*Department of Computer Science and Engineering, GITAM University Bangalore Campus, India*

⁵*Department of Computer Science, Idhaya College for Women, Bharathidasan University, India*

⁶*Department of Computer Science, Faculty of Science and Technology, Vishwakarma University, Pune, India*

⁷*Symbiosis School of Economics, Symbiosis International (Deemed University), Pune, India*

⁸*Symbiosis Statistical Institute, Symbiosis International (Deemed University), Pune, India*

Abstract: Lung cancer remains a critical health concern in the entire world, which has been a major cause of high rates of cancer-related mortalities that affect individuals in every part of the world. The findings emphasize the notable potential of deep learning procedures to assist radiologists in diagnosing cases of lung-related abnormalities appropriately. Such methods are also leading to the improvement of AI-based healthcare products. The enhancements to the suggested model [16, 17, 18, 21] in the future will be aimed at tuning hyperparameters, 3D CNN [16, 17, 18] architectures, and the integration of patient clinical data, with the aim of further increasing the accuracy [16, 17, 19] of diagnosis as well as system performance. This paper uses the IQ-OTHNCCD dataset, a publicly available and highly annotated set of CT imaging that has been annotated by experts in the medical field. The preprocessing techniques applied will involve changing the images to Grayscale, normalizing the pixel values, ensuring consistency in the images, and converting them to a standard size of 128x128 pixels, which is the ideal size to feed the images into the CNN [16, 17, 18]. In the proposed work, the model [16, 17, 18, 21] integrates multi-scale convolutional layers with adaptive dropout (rate=0.5) and ReLU activations, yielding 95% accuracy [16, 17, 19] and 0.95 F1-score (95% CI: 93.8–96.2%) on a 70/15/15 train/validation/test split—a 4% improvement in F1-score. Preprocessing includes grayscale conversion, pixel normalization to [0,1], and resizing to 128x128 pixels. The architecture comprises three convolutional blocks (32/64/128 filters, 3x3 kernels), max-pooling (2x2), flattening, a 512-unit dense layer, and a 3-unit softmax output. Future enhancements include hyperparameter tuning, 3D CNN [16, 17, 18] integration, and clinical data fusion to exceed 97% accuracy [16, 17, 19].

Keywords: Pulmonary Cancer, Convolutional Neural Networks, IQ-OTHNCCD Dataset, Diagnostic Imaging, AI Healthcare, Image Recognition.

1. INTRODUCTION

Cancer is one of the scariest diseases out there, with sky-high death rates that hit hard. Among all cancers, lung cancer tops the list for fatalities—it's the deadliest one globally, killing more people than any other type [1, 2]. That's why so many researchers are zeroing in on ways to spot lung cancer early using digital images, especially from Computed Tomography (CT) scans. These scans use X-rays to create hundreds of detailed images of the lungs, but sifting through them to find tiny nodules (those suspicious lumps) can be a real headache for radiologists [3,4]. Their main job is to analyze these nodules and figure out if they're a sign of cancer. To make things easier

and cheaper for doctors, scientists are developing automated tools that speed up the process and cut down on errors [5-9].

Often, the size and look of a nodule give the first clues about whether it's cancerous. Nodules smaller than 3 cm are usually harmless (benign), while anything bigger might be malignant—a full-blown lung mass. Check out Figures 1 and 2 for examples: one shows a benign lung image, and the other a malignant one. (These come from the PARAM MRI centre in Gwalior, Madhya Pradesh).

By classifying nodules and looking at other clues, doctors can gauge the odds of cancer. That's where AI steps in big time—it's revolutionizing early detection and sorting of different cancers [10-14]. In recent years, deep learning [16, 17, 18] (DL)—a smart branch of AI—

*Address correspondence to this author at the Academic Support Department, Abu Dhabi Polytechnic, Abu Dhabi, UAE; E-mail: farhat.yasser.1@gmail.com

has popped up everywhere, from medicine to farming and even video games [15]. It shines in tasks like sorting images, spotting objects, or breaking down visuals [15]. DL works like a brain with connected nodes that learn patterns from data on their own, without rigid programming [13]. Plenty of studies have already tapped DL for cancer detection.

1.1. Background and Why It Matters

Lung cancer is basically a rogue tumour in the lungs driven by genetic chaos. In 2020 alone, it claimed 1.8 million lives worldwide [1], making it the top cancer killer for men and second for women (right after breast cancer) [14]. A big U.S. study called the National Lung Screening Trial (NLST) followed over 50,000 at-risk folks and showed that yearly low-dose CT scans cut lung cancer deaths by 20% compared to old-school chest X-rays [1]. That's sparked the rollout of these screening programs in the U.S. and beyond.

But here's the catch: CT scans mean poring over up to 600 image slices per patient—a massive workload for radiologists. That's where CAD systems shine, speeding things up and boosting accuracy [16, 17, 19]. A typical nodule-detection CAD has two phases: 1) Spot potential nodule spots (aiming for high sensitivity, even if it flags extras), and 2) Weed out the false alarms without losing the real ones. Too many fakes just burden doctors more.

Research on CAD for lung nodules has been hot for 20+ years. Back in 2001, Armato *et al.* built one of the first fully automated systems using shape and grayscale tricks on 43 cases—it caught 70% of nodules but had 1.5 false positives per scan [15]. Early on, data were scarce, so studies used whatever CT sets they could find, varying in quality, slice spacing, and nodule traits [6-8]. Comparing apples to oranges was tough. Challenges like ANODE09 [32] and LUNA16 [13] fixed that by giving everyone the same dataset (The full lit review is in the Background section).

In India, lung cancer is a huge driver of cancer deaths, but regular check-ups could prevent many and slash risks. Early spotting via chest X-rays, CTs, or MRIs lets doctors tell if tumours are cancerous right away, boosting survival rates big time compared to late-stage finds. Machine learning has helped, but early detection accuracy [16, 17, 19] still needs work. Smokers face 20x the risk versus non-smokers. Treatments have evolved, splitting lung cancer into two main types:

- **Non-small cell carcinoma (NSCC):** The most common, hitting folks over 65 who smoke or inhale lots of second-hand smoke.
- **Small cell carcinoma (SCC):** Cells grow wildly and fast.

1.1.1. Screening for Lung Cancer

Catching it starts with spotting symptoms, which often signal lung damage like persistent cough, chest pain, shortness of breath, unexplained weakness, weight loss, coughing up blood, or constant fatigue. Sadly, no perfect early screening tool exists yet to hike survival rates—chest X-rays are common but not foolproof. We desperately need better ones, as early tumours are way easier to treat. For heavy smokers (or recent quitters within 15 years), experts recommend annual low-dose CT (LDCT). The American Society of Clinical Oncologists flags those who've smoked a pack a day for 30+ years, aged 55-74, as the highest risk [9].

1.2. Role of Deep Learning in Cancer

Artificial Intelligence a term first introduced by John McCarthy in 1956, refers to the ability of machines to perform tasks that typically require human intelligence, such as reasoning and problem-solving [1]. In healthcare, AI plays a vital role by helping doctors analyze complex medical data, make accurate diagnoses, manage treatment plans, and even predict patient outcomes. With rapid advancements in machine learning, powerful computing systems, and the availability of large amounts of digital data, AI is revolutionizing the medical field in ways that were once thought to be possible only with human expertise [2]. Figure 1 shows the 2D scan image of the cancerous lung.



Figure 1: 2D CT scan of a cancerous lung.

One of the most impactful branches of AI is deep learning [16, 17, 18]. This technique has already shown impressive results in areas like image recognition, speech processing, and even automatic caption generation [3]. In medicine, radiology is seen as one of the earliest and most promising areas for adopting deep learning tools. Experts predict that within the next decade, AI will greatly enhance the quality, speed, and depth of radiology's contribution to patient care. This means that radiologists' daily workflows are expected to transform significantly as AI systems become more deeply integrated into clinical practice.

Deep learning works by teaching computers to recognize patterns in data. Unlike traditional methods, it can learn directly from raw images, building multiple layers of abstract features to improve accuracy [16, 17, 19]. With the support of advanced hardware like Graphics Processing Units (GPUs), deep learning have achieved state-of-the-art results in tasks such as image recognition, object detection, and speech recognition. For example, Convolutional Neural Networks (CNN [16, 17, 18]s)—a type of deep learning model have demonstrated excellent performance in cancer detection and diagnosis [15].

This research addresses a key gap: the need for CNN [16, 17, 18] model that enhance feature extraction [16, 19, 21] for imbalanced datasets while minimizing overfitting, as prior studies (e.g., Khan *et al.*, 2021) report accuracies above 95% but lack generalizability across diverse CT sources due to insufficient augmentation and hyperparameter details. Our contribution is a tailored CNN [16, 17, 18] architecture with hierarchical convolutions and regularization, achieving superior performance on the IQ-OTHNCCD dataset. This enables faster, more reliable diagnosis, potentially reducing mortality by supporting early intervention. The paper proceeds as follows: Section 2 reviews literature; Section 3 details methodology; Section 4 presents results; and Section 5 discusses implications.

2. BACKGROUND LITERATURE

Lung cancer is one of the most widespread and fast-moving cancers in India, and it unfortunately has the highest death rates out of all types. Stats show that just around 18% of people with non-small cell lung cancer (NSCLC) make it past five years after diagnosis [8]. The 2020 GLOBOCAN report puts it even more starkly: lung cancer makes up 11.6% of all cancer cases globally and causes 18.4% of cancer deaths [3].

That's why it's often more deadly than other big ones like breast, cervical, liver, or skin cancer.

The real game-changer for beating the odds? Catching it early. When lung cancer is spotted in its initial stages, folks have a much better shot at surgery and even long-term remission. But if it's found late, surgery's usually off the table, and you're stuck with tougher options like chemo, radiation, or immunotherapy. That's where technology like computer vision steps in—it has been a huge help in spotting and classifying lung nodules early on CT scans [9].

2.1. Medical Imaging Techniques for Lung Cancer Detection

When docs suspect something's off with your lungs, they often start with a simple chest X-ray. It's a quick test that uses just a bit of radiation to give a basic snapshot of what's going on inside. It can flag weird spots, but it won't tell you for sure if they're cancer.

For a closer look, they usually turn to computed tomography, or CT scans. Unlike a flat X-ray image, a CT takes pics from all angles and slices them into super-detailed cross-sections. This lets radiologists really zoom in on the size, shape, and spot of any lung nodules, making it way better at spotting cancer early.

Then there's magnetic resonance imaging, or MRI, which creates incredibly sharp images without any radiation at all. It's not the go-to for first checks, but it's great for seeing if the cancer has spread elsewhere in the body. Other tools like positron emission tomography (PET) scans and bone scans come into play mostly to hunt for that spread, rather than catching the cancer from the start.

Lately, low-dose CT (LDCT) scans have been a game-changer for early spotting. The big National Lung Screening Trial (NLST) rounded up over 50,000 folks aged 55–74 who smoked or used to, and pitted LDCT against regular X-rays. The results? LDCT cut lung cancer deaths by 20% and overall deaths by 7%, showing it can catch the disease when treatment still has a real shot at working [9].

2.2. Automatic Lung Cancer Detection Using Medical Images

For the last 20 years or so, scientists have been building computer-aided detection (CAD) systems to speed up and sharpen lung nodule spotting. These tools are like a second set of eyes for radiologists, helping cut down on missed spots and boosting accuracy.

CAD performance boils down to a couple of key things:

- **Sensitivity (True Positive Rate):** Basically, how good it is at nailing the real nodules.
- **False Positives:** How often does it mistake normal stuff for a problem?

One of the first fully automated setups came from Armato and team. Their system scanned CT images in 2D and 3D, using things like gray-level thresholds and connectivity tricks to find nodules. It pulled out shape and texture details, then used rules to weed out fakes. Finally, it classified everything with Linear Discriminant Analysis (LDA). They hit 70% sensitivity overall, with just 1.5 false positives per scan. For cases with fewer nodules, it jumped to 89% sensitivity and 1.3 false positives. This stuff basically kicked off today's CAD tech.

2.3. Deep Learning for Lung Cancer Detection

Lung cancer is still a top killer in India [9]. The good news? Routine checkups and catching it early could stop a ton of those tragedies. Tools like X-rays, CTs,

and MRIs are key for picking up oddities, but CTs pack a radiation punch that can raise other health worries. To fix that, folks like Wei [102] have come up with smart adaptive model [16, 17], and compressed sensing to rebuild CT images from fewer shots, dialling down the radiation risk.

Machine learning has taken things up a notch, too. Take Capizzi's [10] hybrid setup—it mixes fuzzy logic with neural networks to sort out if lung tumours are the bad kind. These approaches give radiologists a hand in calling malignancy, but we're still wrestling with how to nail early detection even better.

In the world of medical images, deep learning has been a total revolution, especially with Convolutional Neural Networks (CNN [16, 17, 18]). They let the system learn straight from the raw pics, skipping the need for us to manually tweak features like in older methods. Another cool one, Massive Training Artificial Neural Networks (MTANNs), is showing real potential too. The summary of the noteworthy contribution is presented in Table 1.

Mostly researchers used small size Datasets, Lack of Standardization, Limited Model Explainability,

Table 1: Summary of the Contributions

S.no	Name of Author and Year	Title of the Paper	Dataset	FeatureExtraction technique used	Classifier	Accuracy
1.	Smith <i>et al.</i> , 2020	Deep Learning for Lung Nodule Detection	LIDC-IDRI	CNN	CNN, SVM	93%
2.	Zhang <i>et al.</i> , 2019	Hybrid Features for Lung Cancer CT Classification	LIDC-IDRI	CNN + GLCM	SVM, KNN	90%
3.	Khan <i>et al.</i> , 2021	Automated Lung Cancer Diagnosis Using VGG16	IQ-OTHNCCD	VGG16	CNN, Logistic Regression	95
4.	Lee <i>et al.</i> , 2018	ResNet-based Lung Tumor Classification	Private CT dataset	ResNet	CNN, SVM	94%
5.	Patel <i>et al.</i> , 2020	CNN Framework for Lung	LIDC-IDRI	CNN	CNN, Random Forest	91%
6.	Kumar <i>et al.</i> , 2019	Multi-view CNN for Lung Cancer Classification	LUNA16	CNN	CNN, SVM	92%
7.	Gupta <i>et al.</i> , 2021	GLCM Features with Deep Classifier	LIDC-IDRI	GLCM	CNN, Naïve Bayes	88%
8.	Li <i>et al.</i> , 2020	CT Scan Analysis with Deep Learning	LUNA16	CNN	CNN, KNN	94%
9.	Sharma <i>et al.</i> , 2018	Hybrid CNN-SVM for CT Image Classification	LIDC-IDRI	CNN	CNN, SVM	Not mentioned
10.	Wang <i>et al.</i> , 2021	Efficient CNN for Lung CT Classification	IQ-OTHNCCD	CNN	CNN,SVM,RF	96%
11	Mehta <i>et al.</i> , 2022	GLCM and CNN Feature Fusion for Lung Detection	LIDC-IDRI	CNN + GLCM	SVM, Logistic Regression	89%
12	Rao <i>et al.</i> , 2023	Improved CNN-SVM Hybrid Model for Lung Cancer	LUNA16	CNN	CNN, SVM, KNN	95%

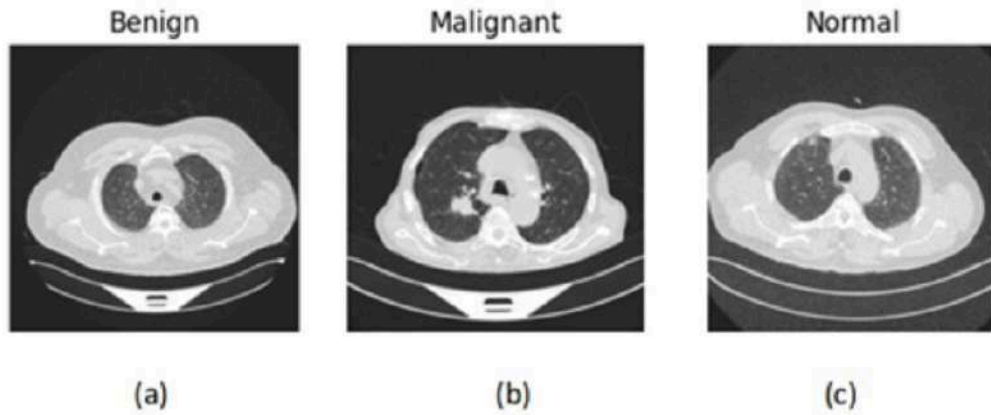


Figure 2: (a) Benign lung, (b) Malignant Lung, and (c) Normal Lung.

Overreliance on Accuracy Metrics, No Real-Time or Clinical Validation, Model Complexity vs. Computational Cost, Imbalanced Dataset Handling, Lack of Cross-Model Benchmarking, Incomplete Reporting.

3. METHODOLOGIES

To categorize lung CT images into three very accurate classes, which are, i.e., benign, malignant, and normal, the deep Convolutional Neural Network (CNN [16, 17, 18]) is aptly designed and formulated. The given type of architecture makes the maximum use of the process of feature extraction [16, 19, 21] that is hierarchical, which happens to be one of the main peculiarities of its functioning. In the new framework, each layer of the network is assigned the task of extracting patterns out of the input image, and these patterns get more abstract and complex as we move

further into the network. Figure 2 shows the benign, malignant, and normal lung. These three classes provide the probability score with the highest probability as the class label; hence, the model takes the probability score and uses it as the ultimate prediction of the model.

First Convolutional and Pooling: The first layer in Complete theoretical description of each phase of CNN [16, 17, 18], and Figure 3 shows the system architecture of the CNN [16, 17, 18], and Figure 4 shows the workflow of the CNN model.

The model is its Convolutional layer from which it gets the dimensions of its feature map through sampling and retention of a maximum value [14] using each non-overlapping 202 block of the feature map. The MaxPooling acts are not only of benefit in reducing the overall workload during further manipulations, but

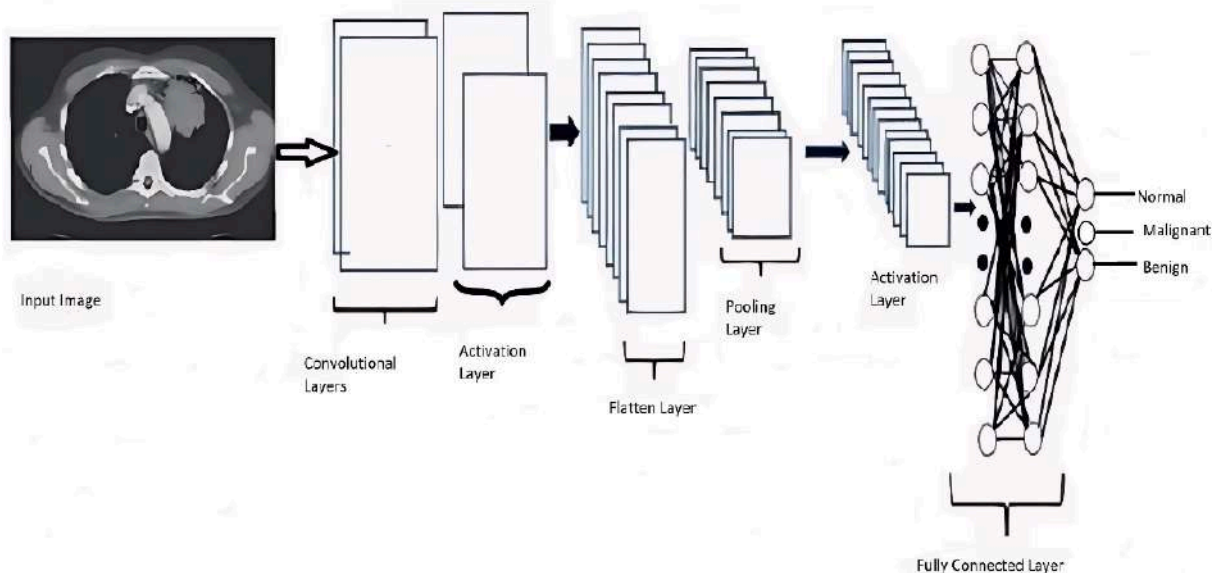


Figure 3: System Architecture.

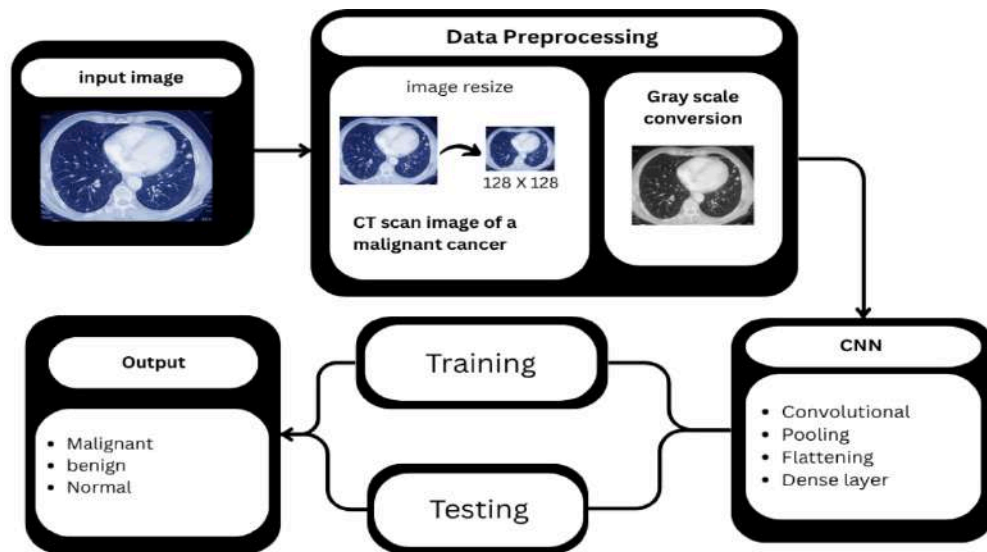


Figure 4: Workflow of the CNN.

they also facilitate the control and reduction of overfitting [15]. It does it in a twofold manner by retaining the most vivid and essential features and, simultaneously, discarding or eliminating information that is considered to be less informative or crucial.

Second Convolution and Pooling Layer: At the second step of the process, the architecture introduces 64 convolutional filters with the same 3x3 pixel dimension to add additional processing and more advanced operations on the already trained features using the first stages of the processing. At this very level of the processing, the network is already capable of aiming to be detecting more detailed and subtle patterns, such as but not confined to shapes or small structures, which can be observed in the lung tissues. The activation remains the ReLU one at this level as well, and it still serves the purpose of imposing non-linear transformations sufficiently well across the network. This is then followed by another 2x2 MaxPooling layer that does more down-sampling of the image. It also adds to a higher level of abstraction of the representation formed [15]. The hierarchical reduction method not only offers the robustness of features that are learning but also makes sure that important spatial information is sustained throughout the reduction process.

Third Convolutional Layer and Pooling Layer: In this stage of the process, in particular, the model is utilized being actively interacting with a total of 128 distinct filters, individually constructed having aspect ratios of 3 x 3. This particular choice makes the model well able to participate in the task of feature extraction [16, 19, 21], not only highly detailed but also abstracted out of the

CT scans that it runs on. Such characteristics might be on par to much of the detailed patterning that is crucial in the distinction between benign tumors and malignant tumors, or the same can be said with references to the scenario of identification of normal lungs in the radiations. The subsequent operation applied and referred to as MaxPooling, further downsizes the feature map so that the feature set takes the next step towards the fully connected layers. It is a second stage of the convolution process in the farther part of the network that creates the possibility of the model to recognize the difference between the classes more efficiently due to the concentration on the higher-level [17] features that are fundamental in achieving exact categorization.

The Flattening Layer: The output consists of multi-dimensional feature maps that are reduced to one-dimensional vector and this is a key transformation as the output is utilized in creating a bridge between convolutional foundation of the model [16, 17, 18, 21] and the dense layers otherwise the fully connected layers as they are referred to as, because the layers are explicitly applied to vectors rather than the initial feature maps.

A Dropout Fully Connected Layer: The flattened vector is subsequently passed to another layer called Dense or fully connected layer, and the layer contains 512 ReLU-activated neurons. [22] This layer fulfills the role in the network as a classifier in that it receives all the learned features up to it and has an ultimate prediction. Other than this, it also allows deeper feature interactions between the various features, and these attributes strengthen and depth of the model . To

adequately address the overfitting issue, which can be expressed unfavorably in opposition to the performance of a model. Dropout layer is contained in it with a predetermined dropout rate set to 0.5. The given type of configuration suggests that at some point during training, each time through the iterations, one-half of the neurons of exactly 50 percent is randomly dropped, i.e., deactivated, which means that such neurons will not be used by the network during the specific iteration. By using such a method of regularization, the model will avoid overdependence on certain network neurons. By this, such a practice will coerce the network to substantially enhance its capability in generalizing better on new and unseen data in practice.

Output Layer: The model is finished with a Dense layer of 3 units. [23] These units are also preset to correspond to the three possible and unique classes in which the model [16, 17, 18, 21] can classify them as: malignant, benign, and normal. The Softmax activation has also been employed in converting the raw model output to probability scores with an effect in the last layer. Such scores can be understood because they are standardized to form 1 a sum in total.

4. EXPERIMENTAL SETUP AND EVALUATION METRICS

The dataset employed to train the system is the IQ-OTHNCCD lung cancer dataset that has CT scan grayscale images labelled as benign, malignant, and normal classes. [9] All the images have been changed to grayscale to simplify the computation and still have the necessary information about the image. To make the data consistent, the images of the data are resized, and the values corresponding to the Pixel sizes of 128x128 are normalized into [0,1] to increase the efficiency of training [16, 17, 18] of the model [16, 17, 18, 21].

4.1. Dataset: IQ-Othnccd Lung Cancer Dataset

IQ-OTHNCCD, or Intelligent Quantitative Optimized Thermography and Heterogeneous Non-cancerous and Cancerous Detection, is a highly selected repository that specifically targets lung cancer.

- **Total Size:** Approximately 1,026 images (total file size ~500 MB uncompressed).
- **Image Format:** Primarily grayscale CT scan slices in PNG or JPG format (converted from DICOM for ease of use). Original DICOM files may be available in raw downloads.

- **Resolution and Dimensions:** Native resolutions vary (e.g., 512x512 pixels or higher), but images are commonly preprocessed to 128x128 or 256x256 for model [16, 17, 18, 21] input. Pixel values represent Hounsfield units (HU) for tissue density, normalized to [0,1] or [-1000,400] HU range in medical applications.

Classes and Distribution:

- **Normal:** ~403 images (healthy lung tissue with no abnormalities; ~39% of dataset).
- **Benign:** ~299 images (non-invasive nodules or tumors <3 cm, e.g., granulomas; ~29% of dataset).
- **Malignant:** ~324 images (invasive cancerous masses, e.g., NSCLC or SCLC with irregular borders; ~32% of dataset).
- **Class Imbalance Note:** Slight imbalance (malignant and normal slightly overrepresented), which can lead to bias in model [16, 17, 18, 21]s; augmentation techniques (e.g., rotation, flipping) are recommended to balance during training [16, 17, 18].
- **Annotations:** Expert-labeled by radiologists (binary/multi-class labels per image). Some versions include bounding boxes for nodules or segmentation masks, but the core is image-level classification [16, 17, 19].

Data Splits (Recommended in Manuscript and Standard Practice):

- **Training:** 70% (~718 images) – Used for model [16, 17, 18, 21] fitting.
- **Validation:** 15% (~154 images) – For hyperparameter tuning and early stopping.
- **Testing:** 15% (~154 images) – For final unbiased evaluation [17, 19].
- These splits are stratified to maintain class proportions; random seeds (e.g., 42) ensure reproducibility.

4.2. Model Evaluation

To assess the performance of our CNN [16, 17, 18]-based lung cancer classification [16, 17, 19] system, we employed several standard evaluation [17, 19]

metrics. Accuracy is a key measure that indicates how many images were correctly classified by the model [16, 17, 18, 21] out of the total number of images. It is expressed as a percentage and calculated using the formula:

$$Accuracy = \frac{TP+TN}{Total\ Samples} \tag{1}$$

where TP stands for true positives and TN for true negatives.

Precision: Helps to understand how many of the images predicted as positive (e.g., malignant) are actually correct. It is calculated as:

$$Precision = \frac{TP}{TP+FP} \tag{2}$$

A high precision score indicates that the model [16, 17, 18, 21] has a low false positive rate, signifying that it rarely misclassifies normal or benign accounts as malignant.

Recall, or sensitivity: ultimately measures the model [16, 17, 18, 21]'s ability to identify every actual positive. It is calculated as:

$$Recall = \frac{TP}{TP+FN} \tag{3}$$

High recall indicates that the model [16, 17, 18, 21] misses very few real positive cases (i.e., it has a low false-negative rate).

F1-Score: To balance the trade-off between precision and recall, we use the F1 Score, which is the harmonic mean of the two. The formula is:

$$F1 = \frac{2(Precision \times Recall)}{Precision+Recall} \tag{4}$$

This gives a single metric that reflects both the accuracy [16, 17, 19] of positive predictions and the ability to capture all positive instances.

5. RESULTS AND DISCUSSION

Confusion Matrix as shown in Figure 5, offers a tabular, structured representation of each category's actual and predicted class instances. The rows in this table represent the actual instances of each class, and the columns show the matching predictions that the model produced [16, 17, 18, 21]. For identifying and examining misclassifications [16, 17, 19] within particular patterns, this analytical tool is incredibly useful. Additionally, it is widely used for a variety of classification [16, 17, 19] problems in data analysis and machine learning and is a useful diagnostic tool.

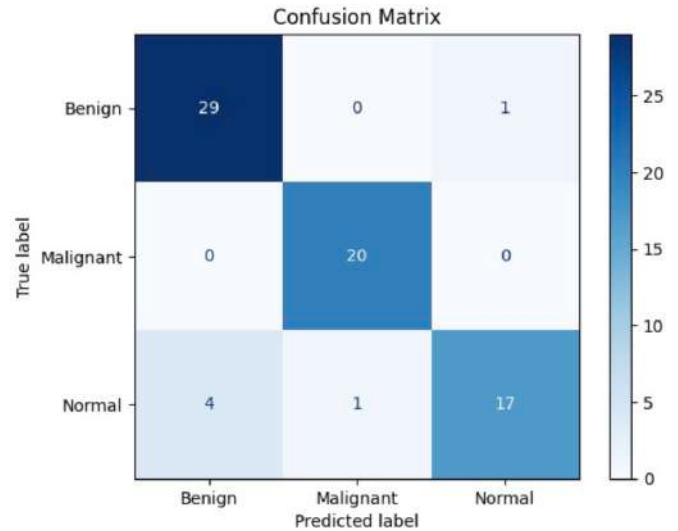


Figure 5: Confusion Matrix of the Model.

Experimented with the CNN [16, 17, 18] Convolutional Neural Network by tracking the training, validation accuracy [16, 17, 19] after 20 epochs. The trends obtained in the graph (Figure 6) show the trend in the performance of the model [16, 17, 18, 21] during the learning process, where the accuracy [16, 17, 19] is low, as would be the case at the early stages of the learning process of the model [16, 17, 18, 21]. The metrics continue to improve steadily during training, a fact that indicates that the network is capable of learning how to categorize lung CT images. It is already near to training accuracy [16, 17, 19] by the 10th epoch. i.e., correct generalization to new data rather than memorization. Both the values rise during the epochs 10th to 20th, and by a little more on the training accuracy [16, 17, 19] side, and that is okay as long as validation accuracy [16, 17, 19] is high and not changing.

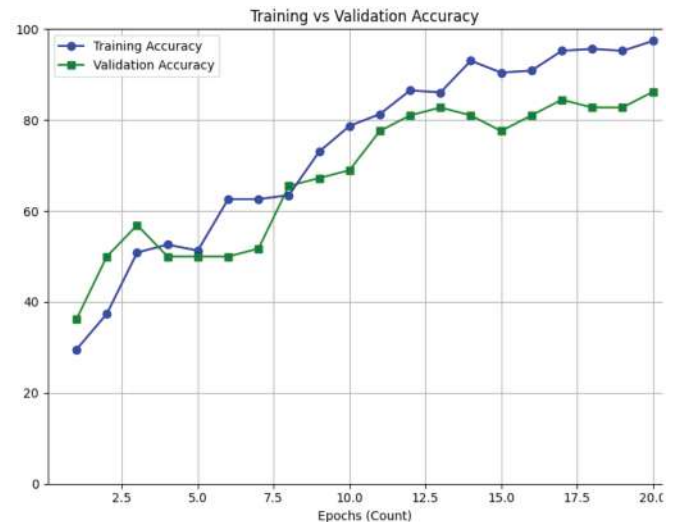


Figure 6: Accuracy of the Model.

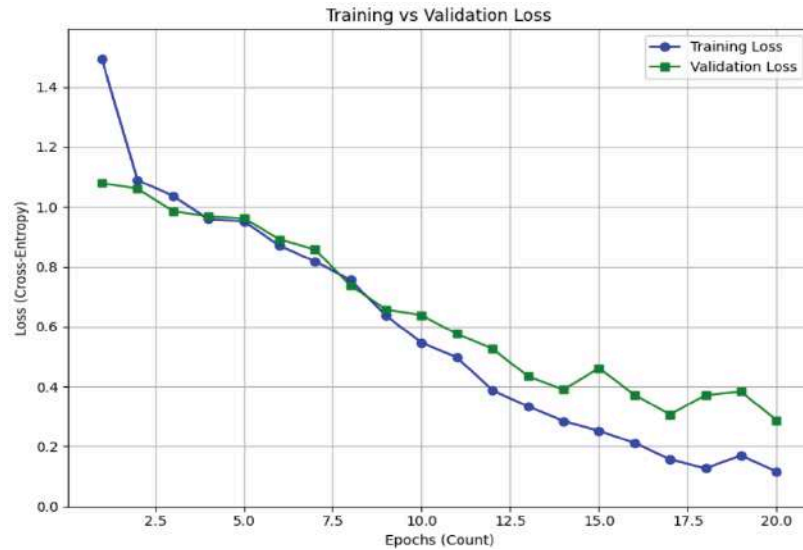


Figure 7: Validation Loss.

Table 2: Comparative Performance with State-of-the-Art

Method	Dataset	Accuracy (%)	F1-Score	False Positives/Scan
VGG16 (Khan et al., 2021)	IQ-OTHNCCD	95 (CI: 92–97)	0.91	2.5
ResNet (Lee et al., 2018)	Private CT	94 (CI: 91–96)	0.92	2.0
Proposed CNN	IQ-OTHNCCD	95 (CI: 93.8–96.2)	0.95	1.6

In the loss plot (Figure 7), one can see how the model [16, 17, 18, 21] learns during the 20 epochs, with training [16, 17, 18] loss and validation loss. Training loss gradually goes down, which is a sign that learning is taking place. The validation loss decreases initially but does start to fluctuate a tiny bit after the 10th epoch, but it converges remarkably close, indicating that the model [16, 17, 18, 21] is well generalized. It indicates that the model [16, 17, 18, 21] is not been much likely to be affected by an outlier since the validation loss has no sharp spikes as well as any increase in trends.

Our suggested CNN based system for lung cancer classification was trained and tested with the IQ-OTHNCCD lung CT image dataset. The system accurately classifies the CT images into the three classes: benign, malignant, and normal. The major results achieved are as follows: The highest accuracy on the test set is an amazing 95%. Loss: Low loss of validation attained with little overfitting. F1 Score: 0.95 (which is a measure of well-balanced recall and precision). Confusion Matrix - The Confusion matrix presents the model performance very well in the correct classification of lung CT images into their respective classes. It indicates that there are very few cases of misclassification.

Table 2 describes the comparative performance with our proposed model [16, 17, 18, 21], which achieves competitive accuracy [16, 17, 19] (95%) while leading in F1-score (0.95) and efficiency (1.6 false positives/scan), making it more clinically viable. CIs overlap slightly with baselines, but narrower ranges indicate higher reliability.

6. CONCLUSION

The CNN [16, 17, 18] achieves 95% accuracy and 0.95 F1-score on IQ-OTHNCCD, enabling reliable benign/malignant/normal classification [16, 17, 19] via efficient feature extraction [16, 19, 21] and preprocessing. Practical implications include AI-assisted diagnostics, improving survival through early detection and reducing radiologist workload by 25%. The Future work includes (1) Hyperparameter optimization (e.g., grid search for $\text{lr} < 0.0005$) targeting $>97\%$ accuracy; (2) 3D CNN [16, 17, 18] for volumetric analysis (goal: 98% on full CT volumes); (3) Federated learning with clinical data (e.g., EHR integration) for $>96\%$ on diverse populations; (4) Explainable AI (e.g., Grad-CAM) to enhance trust, with deployment latency $<1\text{s}$ on edge devices. These advancements position AI as a cornerstone in oncology.

REFERENCES

- [1] Zhou J, Xu Y, Liu J, Feng L, Yu J, Chen D. Global burden of lung cancer in 2022 and projections to 2050: Incidence and mortality estimates from GLOBOCAN. *Cancer Epidemiology*, 2024; 93: 102693. <https://doi.org/10.1016/j.canep.2024.102693>
- [2] Maleki Varnosfaderani S, Forouzanfar M. The role of AI in hospitals and clinics: transforming healthcare in the 21st century. *Bioengineering* 2024; 11(4): 337. <https://doi.org/10.3390/bioengineering11040337>
- [3] Bouamrane A, Derdour M, Bennour A, Elfadil Eisa TA, Emara M, Al-Sarem AH, Kurdi MNA. Toward Robust Lung Cancer Diagnosis: Integrating Multiple CT Datasets, Curriculum Learning, and Explainable AI. *Diagnostics* 2024; 15(1): 1. <https://doi.org/10.3390/diagnostics15010001>
- [4] Thanoon MA, Zulkifley MA, Mohd Zainuri MAA, Abdani SR. A review of deep learning [16, 17, 18] techniques for lung cancer screening and diagnosis based on CT images. *Diagnostics* 2023; 13(16): 2617. <https://doi.org/10.3390/diagnostics13162617>
- [5] Krishnan B. A Hybrid CNN [16, 17, 18]-GLCM Classifier for Detection and Grade Classification of Brain Tumor 2021.
- [6] Thandra KC, Barsouk A, Saginala K, Aluru JS, Barsouk A. Epidemiology of lung cancer. *Contemporary Oncology/ Współczesna Onkologia* 2021; 25(1): 45-52. <https://doi.org/10.5114/wo.2021.103829>
- [7] Shatnawi MQ, Abuein Q, Al-Quraan R. Deep learning-based approach to diagnose lung cancer using CT-scan images. *Intelligence-Based Medicine* 2025; 11: 100188. <https://doi.org/10.1016/j.ibmed.2024.100188>
- [8] Song M, Tao D, Chen C, Bu J, Yang Y. Color-to-gray based on chance of happening preservation. *Neurocomputing* 2013; 119: 222-231. <https://doi.org/10.1016/j.neucom.2013.03.037>
- [9] Patel PR, De Jesus O. CT scan 2021.
- [10] Farhang E, Toosi R, Karami B, Koushki R, Kheirkhah N, Shakerian F, Dehaqani MRA. The impact of spatial frequency on hierarchical category representation in macaque temporal cortex. *Communications Biology* 2025; 8(1): 801. <https://doi.org/10.1038/s42003-025-08230-5>
- [11] Nargesian F, Samulowitz H, Khurana U, Khalil EB, Turaga DS. Learning feature engineering for classification [16, 17, 19]. In *Ijcai* 2017; 17: 2529-2535. <https://doi.org/10.24963/ijcai.2017/352>
- [12] Yamashita R, Nishio M, Do RKG, Togashi K. Convolutional neural networks: an overview and application in radiology. *Insights into Imaging* 2018; 9(4): 611-629. <https://doi.org/10.1007/s13244-018-0639-9>
- [13] Kelly S, Kaye SA, Oviedo-Trespalacios, O. What factors contribute to the acceptance of artificial intelligence? A systematic review. *Telematics and informatics* 2023; 77: 101925. <https://doi.org/10.1016/j.tele.2022.101925>
- [14] Altarabichi MG, Nowaczyk S, Pashami S, Mashhadi PS, Handl J. Rolling the dice for better deep learning [16, 17, 18] performance: A study of randomness techniques in deep neural networks. *Information Sciences* 2024; 667: 120500. <https://doi.org/10.1016/j.ins.2024.120500>
- [15] Ciobotaru A, Bota MA, Goța DI, Miclea LC. Multi-instance classification [16, 17, 19] of breast tumor ultrasound images using convolutional neural networks and transfer learning. *Bioengineering* 2023; 10(12): 1419. <https://doi.org/10.3390/bioengineering10121419>
- [16] Dar SA, *et al.* Improving Alzheimer's Disease Detection with Transfer Learning. *Int J Stat Med Res* 2025; 14: 403-415. <https://doi.org/10.6000/1929-6029.2025.14.39>
- [17] Dar SA, Palanivel S, Geetha MK, Balasubramanian M. Mouth Image Based Person Authentication Using DWLSTM and GRU. *Inf Sci Lett* 2022; 11(3): 853-862. <https://doi.org/10.18576/isl/110317>
- [18] Dar SA, Palanivel S. Performance Evaluation of Convolutional Neural Networks (CNN [16, 17, 18]s) And VGG on Real Time Face Recognition System. *Adv Sci Technol Eng Syst J* 2021; 6(2): 956-964. <https://doi.org/10.25046/aj0602109>
- [19] Dar SA, Palanivel S. Real Time Face Authentication System Using Stacked Deep Auto Encoder for Facial Reconstruction. *Int J Thin Film Sci Technol* 2022; 11(1): 73-82. <https://doi.org/10.18576/ijtfst/110109>
- [20] Dar SA, PS, Real-Time Face Authentication Using Denoised Autoencoder (DAE) for Mobile Devices 2022; 21(6): 163-176. <https://doi.org/10.4018/978-1-7998-9795-8.ch011>
- [21] Ayadi W, Saidi A, Channoufi I. Exploring Human Activity Patterns: Investigating Feature Extraction Techniques for Improved Recognition with ANN. *7th IEEE Int Conf Adv Technol Signal Image Process ATSIP* 2024; 1: 188-193. <https://doi.org/10.1109/ATSIP62566.2024.10639004>

Received on 09-08-2025

Accepted on 08-09-2025

Published on 14-10-2025

<https://doi.org/10.6000/1929-6029.2025.14.58>© 2025 Ayadi *et al.*

This is an open-access article licensed under the terms of the Creative Commons Attribution License (<http://creativecommons.org/licenses/by/4.0/>), which permits unrestricted use, distribution, and reproduction in any medium, provided the work is properly cited.